74255

High-Ti Basalt
737.6 g, 13 x 7 x 6 cm

INTRODUCTION

79255 has been described as a medium dark gray, intergranular, homogeneous basalt (Apollo 17 Lunar Sample Information Catalog, 1973). Many zap pits are present on B, with none on any other faces. Approximately 10% of the surface is covered with vugs of 2-3mm diameter. These are lined with crystals of pyroxene, plagioclase, ilmenite, and rarely olivine. The surface texture is variable - T, N, S, E, and W are ha.ckly, B is rounded. The overall shape is angular but irregular (Fig. 1), with one major penetrative fracture parallel to N, with many smaller fractures parallel to it.

This sample was collected from Station 4.

PETROGRAPHY AND MINERAL CHEMISTRY

This sample has been described in detail by several authors. These descriptions are reproduced below.

Apollo 17 Lunar Sample Information Catalog (1973): (description by Agrell) 74255,7 was described as a coarse-grained olivine basalt or diabase. The thin section is comprised of 5% olivine, 33% plagioclase, 46% pyroxene, 5% armalcolite, 10% ilmenite, < 0.5% spinel, < 0.5% native Fe, < 0.5% troilite, and < 1 % matrix. Olivine occurs as rounded (resorbed) crystals where it is in pyroxene, although discrete olivines are present. The only inclusion is possibly one brown spinel. Plagioclase forms lathy crystals, some in coarse sheaves intergrown with pyroxene or with hypidiomorphic pyroxene between crystals (Fig. 2). A few pyroxenes are larger allotrio-morphic crystals with coarsely skeletal outgrowths. These may exhibit a jagged mosaic of blocks with slightly varying extinction, and simulate sector structure in some orientations. The pyroxene is faintly pink with strong dispersions, birefringence increasing at

Figure 1: Hand specimen photograph of 74255.

Figure 2: Photomicrograph of 74255. Field of view is = 2.5 mm.

margins and + 2V in the core of about 20 It is probably calcic pigeonite zoned to ferroaugite. The bulk of the pyroxene is in hypidiomorphic crystals, often in groups of 3 or 4 having a nearly common orientation. These are intergrown with, or interstitial to the plates of plagioclase (Fig. 2). Armalcolite is confined to the central portions of the larger pyroxene crystals. Ilmenite is largely in skeletal embayed plates. It exhibits spinel and rutile exsolution in thin lamellae or discs. Rounded drop-like areas (~30u) occur in the larger ilmenites; these may be accidental due to cutting embayments or true inclusions of weakly reflecting silicate or possibly glass as isolated metal droplets are present in some. Residual mesostasis in small amounts occurs locally; it is composed of acid glass with dark droplets (~1u). Small patches of orthoclase and cristobalite may also occur in the interstices between major minerals. 74255,7 is texturally homogeneous. A few large allotriomorphic pyroxene plates occur with coarse skeletal outgrowths with plagioclase tablets (Fig. 2). The major portion is composed of tabular plagioclase, in which pyroxene crystals are included or occur interstitially (plagioclase-poikilitic). These pyroxenes are hypidiomorphic and may occur in groups of 4 or 5 crystals in sub-parallel orientation.

Dymek et al. (1975):
These authors described 74255 as a medium- to coarse-grained vesicular porphyritic basalt comprised of plagioclase (28%), pyroxene (51%), ilmenite (15%), olivine (4%), and SiO_2 (1%) with minor amounts of armalcolite troilite, native Fe, Cr-ulvospinel, Ca-phosphate, and mesostasis. It strongly resembles 71055 in texture and mineralogy, except that 79,255 is distinctly porphyritic and less vesicular. 74255 is a variant of the plagioclase-poikilitic ilmenite basalts. The results of an electron microprobe point count of polished thin section 74255,61 are presented in Table 1. Olivine occurs principally as tiny (20-10012) cores within pyroxene. A few large grains (up to 0.7mm) have only a narrow pyroxene rim. In addition, two of these grains (~ FO_{70}), without any pyroxene overgrowth, project into a vug. This relationship suggests the existence of a vapor phase early in the crystallization history of this rock. A few rare inclusions of ilmenite and Cr-ulvospinel occur in olivine. The measured range in composition of the olivine is FO_{80-67}. The minor-element abundances and patterns resemble those in 70215 and 71055. The most striking occurrence of pyroxene is as coarse, commonly composite, complexly zoned phenocrysts (up to 4mm across). These range from pale pink to dark pink. Abundant inclusions of ilmenite, together with rare grains of armalcolite and euhedral Cr-ulvospinel, are present. These pyroxenes have measured compositions that range from $Wo_{30}En_{52}Fs_{18}$ to

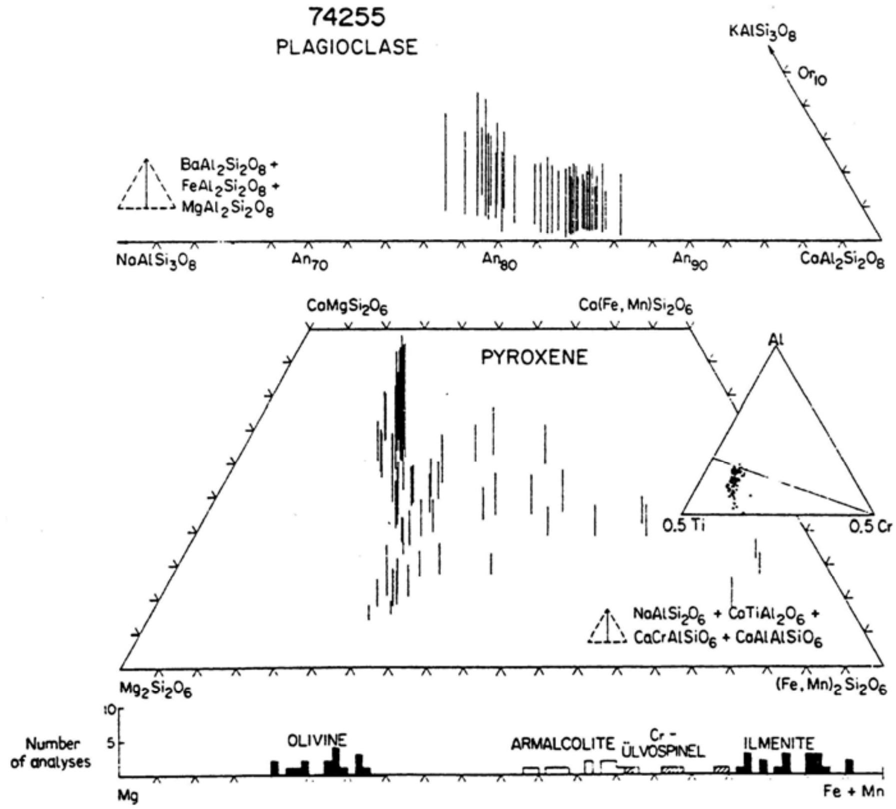

Figure 3: Compositions of the principal silicate and oxide phases in mare basalt 74255. After Dymek et al. (1975).

$W0_{44}En_{40}Fs_{16}$, represented by the high-Ca cluster on Figure 3. The principal variation is in Ca content, with only a slight change in Fe/Mg. The outer portions of some phenocrysts are pigeonite with compositions near $Wo_{10}En_{60}Fs_{30}$. These can be seen to zone continuously to augite (~ $W0_{25}En_{5O}Fs_{25}$)' Hourglass structures are developed in some grains, and microprobe traverses demonstrate the presence of sector zoning. Pyroxene also occurs as colorless to pale pink blocky grains (5-50u) that are poikilitically enclosed by plagioclase. These grade to elongate pyroxene blades that are intergrown with plagioclase and ilmenite. Intergrowths of acicular pyroxene and plagioclase also occur. As shown in Figure 3, the compositions of these pyroxene types fall along an intermediate-Ca trend ($Wo_{1O}En_{60}Fs_{30}$-$Wo_{80}En_{43}Fs_{27}$-$W0_{25}En_{32}Fs_{48}$). Some pyroxenes exhibit extensive Fe enrichment, and one grain has measured compositions that zone from $W0_{35}En_{33}Fs_{32}$ to $Wo_{11}En_{14}FS_{75}$. The Ti/Al ratio closely approaches 1:2 except for aluminous titanaugite, which has excess Al. The relative amounts of AI-Ti-Cr (inset Fig. 3) are consistent with the presence of AI^{VI} and Ti^{3}+. Rare grains of armalcolite [Fe/ (Fe + Mg) = 0.53-0.6]. in part mantled by ilmenite, occur as equant to elongate inclusions (20-50u) in the pyroxene phenocrysts. Euhedral Crulvospinel [-5-25u; Fe/(Fe + Mg) = 0.66-0.80]. occurs as inclusions in olivine and also in the pyroxene that surrounds the olivine. Ilmenite occurs both as inclusions in pyroxene phenocrysts (and rarely olivine), and also intergrown with pyroxene and plagioclase. There is a correlation between the Fe/(Fe+ Mg) ratio of ilmenite and its occurrence: rims on armalcolite ~0.82; inclusions in pyroxene phenocrysts ~0.84-0.87; intergrown with plagioclase and pyroxene ~ 0.86-0.96. Plagioclase ranges in composition from An_{43-85}, and occurs as elongate laths intergrown with pyroxene and ilmenite (up to 200u wide), and as larger irregularly shaped poikilitic grains enveloping pyroxene. Normal zoning (up to 6 mole% An) was observed in several grains. 74255 contains curious intergrowths of plagioclase and SiO_2. This plagioclase is the most sodic in the rock (An_{73-76}; 0.19-0.33 wt%

K_2O). FeO and Fe /(Fe + Mg) increase and MgO decreases with decreasing An content in the plagioclase. The Fe/ (Fe + Mg) of the earliest-formed plagioclase (~ 0.4) is slightly higher than that of the pyroxene that crystallized at this time [i.e., a pigeonite with Fe/(Fe + Mg) ~0.30-0.35]. The presence of armalcolite and spinet only within pyroxene phenocrysts and olivine suggests that these phases formed earliest in the crystallization sequence. Olivine crystallized next, reacting with the melt to form augite before armalcolite ceased crystallization. The presence of euhedral, unreacted armalcolite within a pyroxene phenocryst suggests that pyroxene began to crystallize slightly before ilmenite. Augite phenocrysts continued to grow with ilmenite, and with the onset of plagioclase crystallization, pigeonite nucleated. An augite-series and a pigeonite-series co precipitated with plagioclase and ilmenite to the final stages. Fe-rich pyroxene, SiO_2, sodic plagioclase, and potassic mesostasis formed last. Brown et al. (1975) examined thin section 74255,54 as a Type IB Apollo 17 high-Ti basalt. These authors reported the following modes for 74255,54: olivine 3.2%, opaques 28.3%, plagioclase 18%, clinopyroxene 48.6%, silica 0.1%, mesostasis 1.8%. No detailed description of the petrography and mineral chemistry was given by these authors. Pearce and Timms (1992) used interference imaging to examine plagioclase in 74255, and found no appreciable zoning.

WHOLE-ROCK CHEMISTRY

Detailed whole-rock analyses have been reported by Rose et al. (1975), Shih et al. (1975) (trace elements only), and Rhodes et al. (1976) (major elements only). These are presented in Table 2. 74255 is classified as a Type C Apollo 17 high-Ti basalt, using the scheme of Rhodes et al. (1976), and Warner et al (1979). Rose et al. (1975) reported a

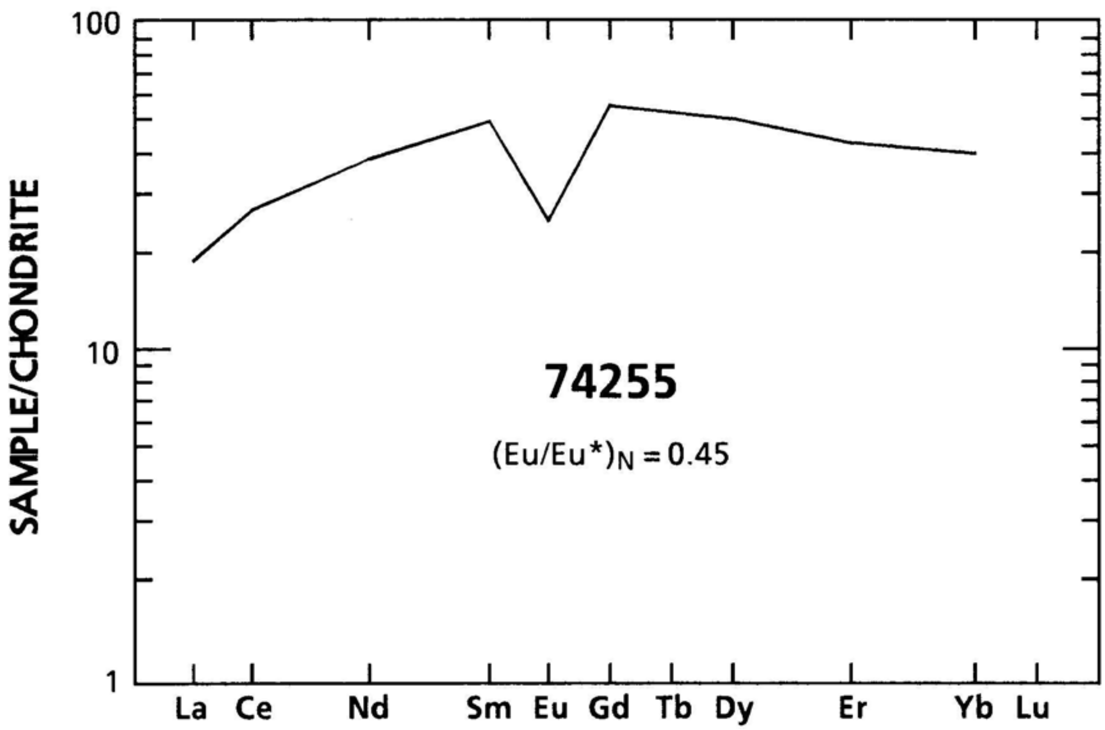

Figure 4: Cho ndrite -normalized rare-earth-element profiles of 74255.

TiO_2 content of 12.76 wt% for 74255,42 with a MG# of 51.5, whereas Rhodes reported 12.17 wt% TiO_2 with a MG# of 50.8 for 74255,25. The REE profile was presented by Shih et al. (1975) (Fig. 4). It is LREE-depleted with a maximum at Gd. The HREE exhibit a slight decrease (relative to chondrites), but are still elevated relative to the LREE-depleted. A negative [(Eu/Eu*) N = 0.45]. Gibson et al. (1976) reported the whole-rock sulfur abundance of 74255 as 1625±30 µgS/g with an equivalent wt% Fe^{o} of 0.210.

RADIOGENTIC ISOTOPES

The Rb-Sr isotopic composition of'74255 has been reported by Barisal et al. (1975), Nyquist et al, (1975, 1976), and Murthy and Coscio (1976) (Table 3). Barisal et al. (1975) and Nyquist et al. (1975) reported the same analyses. Both Nyquist et al. (1976) and Murthy and Coscio (1976) constructed isochrons for 74255 (Fig. 5 a,b) which yielded ages (3.83 ± 0.06 Ga and 3.70 ± 0.12 Ga, respectively) and initial $^{87}Sr/^{86}Sr$ ratios (0.69924 ± 3 and 0.69920 ± 7, respectively) within error of each other. Nyquist et al. (1976) noted that 74255 and 74275, both Type C Apollo 17 high-Ti mare basalts, had identical isochron ages (Fig. 5a). Nunes et al. (1974) undertook a detailed study of the U-Th-Pb isotopic composition of 74255 (Table 4). These authors noted that Type C basalts appeared to have lower $^{206}Pb/^{238}U$ and $^{207}Pb/^{235}U$ ratios than other Apollo 17 mare basalts. Paces et al. (1991) used 74255 data as part of the comprehensive isotopic study of the Apollo 17 site.

EXPOSURE AGE AND COSMOGENIC RADIONUCLIDES

Three studies have reported the exposure age of 74255. Eberhardt et al. (1975) reported a 38Ar-37Ar exposure age of 25 ±3 Ma, and an ^{81}Kr-Kr exposure age of 17.3 ± 1.0 Ma. These authors also reported values of the various Kr isotopic ratios. Eugster et al. (1977) reported an ^{81}Kr-Kr exposure age for 74255 of 17.2± 1.4 Ma, and also the He, Ne, Ar, Kr, and Xe isotopic ratios for this sample. Morgelli et al. (1977) reported exposure ages for 74255 determined by He, Ne, Ar, Kr, and Xe methods and found the ages thus determined were approximately the same (17.3-18.4 Ma). The abundances in 74255 of the various isotopes of the gases used in determining the exposure age were reported by all three works cited above (Table 5). It appears that Eugster et al. (1977) and Morgelli et al. (1977) have reported the same analysis.

EXPERIMENTAL STUDIES

High-Ti mare basalt 74255 has been used in three experimental studies. Bell et al. (1975) conducted a study of spinel/pyroxene symplectites in lunar basalts and used 74255 as part of their study. O'Hara and Humphries (1975) used 74255 to study the conditions required for armalcolite crystallization, and Usselman et al. (1975) used experimental evidence to conclude that basalt 74255 cooled at a rate of 1-3°C/hour.

PROCESSING

The original sample, 74255,0 has been entirely subdivided. The largest remaining samples are : 74255,2 (~128g);,14 (~1208); ,22 (~ 57g); and,38 (~1358). Twelve thin sections have been made of 74255. These are ,7 and ,52-,62.

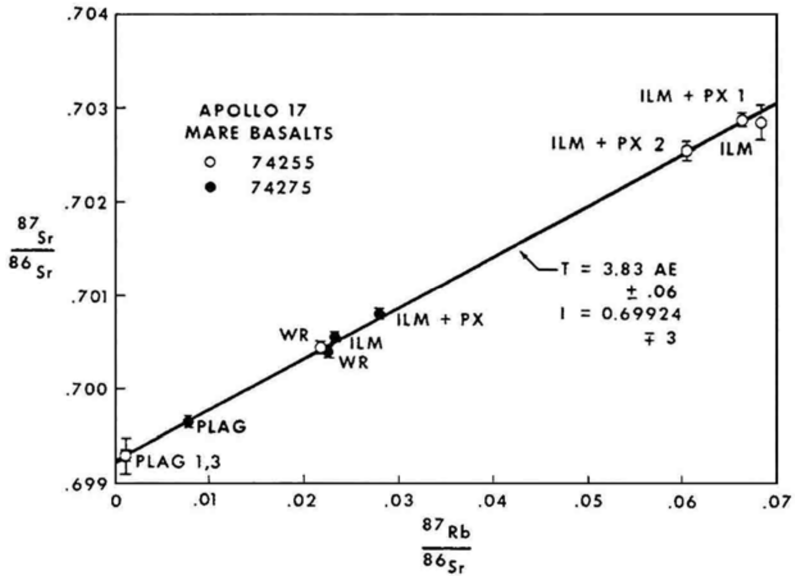

Figure 5a: Mineral separate data for 74255,25 and 74275,56. The mineral isochron shown in the figure is for 74255 data only. Uncertainties are 2a values from the York (1966) program. 74275 data are completely consistent with this isochron and independently define I= 0.69923±0.00010 and T = 3.81±0.32 A.E. After Nyquist et at. (1976).

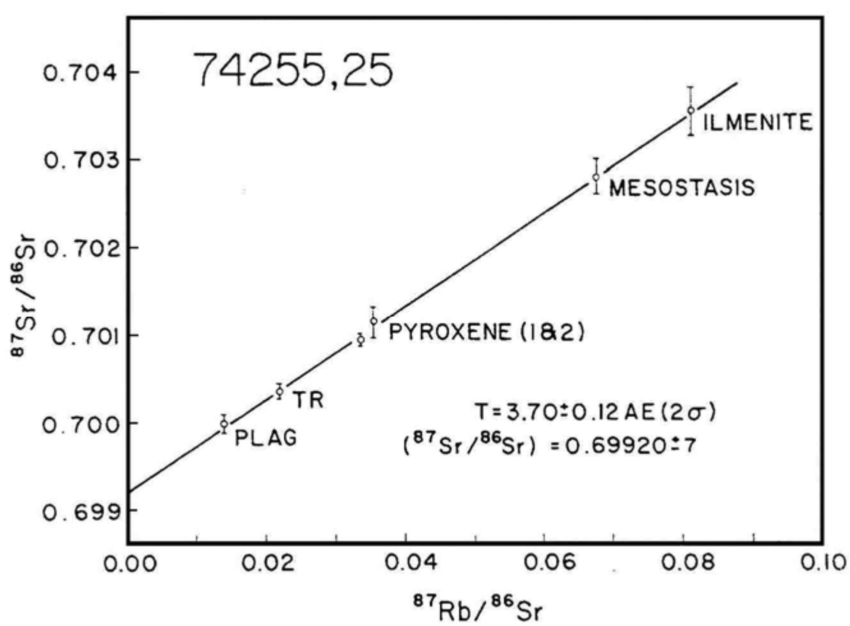

Figure 5b: Rb-Sr internal isochron for 74255,25. Errors for $^{87}Rb/^{86}Sr$ are ±2%, errors for $^{87}Sr/^{86}Sr$ are as noted in Table 1. Best fit line obtained by York-type of weighted regression analysis, with 20 errors. After Murthy and Coscio (1976).

Table 1: 74255: phase abundances, "average" phase compositions and bulk-chemical composition. After Dymek et al. (1975).

	Plag.	Low-Ca pyx	Med-Ca pyx	High-Ca pyx	Fe pyx	Olivine	Ilmenite	Armal.	Cr Ulvöspinel	Fe metal*	Troilite*	Ca phosphate†	SiO_2	Mesostasis	Bulk Composition	
vol.%	$27.6_1 \pm$	$12.3_9 \pm$	$26.1_9 \pm$	$12.3_0 \pm$	$0.9_4 \pm$	$3.2_1 \pm$	$14.5_7 \pm$	$0.5_9 \pm$	$0.1_2 \pm$	$0.0_9 \pm$	$0.1_5 \pm$	$0.0_6 \pm$	$1.0_6 \pm$	$0.7_1 \pm$	Calc.	Rose
	1.2_8	0.8_5	1.2_4	0.8_5	0.2_4	0.4_4	0.9_3	0.1_9	0.0_8	0.0_7	0.0_9	0.0_6	0.2_5	0.2_0	(1695	et al.
wt.%	22.2_3	12.4_6	26.1_8	12.2_2	0.9_6	3.3_5	19.8_9	0.8_1	0.1_6	0.2_1	0.2_1	0.0_6	0.7_3	0.5_2	Pts.)	(1975)
P_2O_5	n.a.	n.a.	n.a.	n.a.	n.a.	n.a.	n.a.	n.a.	n.a.	n.a.	n.a.	43.15	n.a.	0.37	0.03	0.06
SiO_2	47.49	51.70	49.93	47.84	49.39	37.36	0.01	0.07	0.11	n.a.	n.a.	–	97.20	68.27	38.71	38.40
TiO_2	0.32	1.34	2.35	3.46	1.15	0.11	53.58	73.15	20.40	<0.01	0.04	–	0.34	0.90	12.58	12.76
Al_2O_3	32.70	1.76	3.04	4.90	1.22	<0.01	0.07	2.12	8.43	n.a.	n.a.	–	0.95	13.77	9.02	8.84
Cr_2O_3	n.a.	0.46	0.75	0.80	0.29	0.20	1.08	1.59	25.00	n.a.	n.a.	–	n.a.	0.02	0.63	0.60
MgO	0.27	19.82	17.59	14.88	11.08	35.80	2.04	6.20	7.93	0.01	<0.01	–	n.a.	0.27	10.73	0.72
CaO	17.03	6.24	12.22	18.56	9.77	0.27	n.a.	n.a.	n.a.	<0.01	0.02	54.54	0.26	3.98	10.19	10.20
FeO	0.43	19.27	13.78	8.97	27.01	27.00	42.88	17.35	37.48	99.42	63.65	–	0.38	4.85	17.56	17.98
MnO	n.a.	0.33	0.26	0.25	0.37	0.22	0.40	0.16	0.56	n.a.	n.a.	–	n.a.	0.08	0.23	0.28
BaO	<0.01	n.a.	n.a.	n.a.	n.a.	n.a.	n.a.	n.a.	n.a.	n.a.	n.a.	–	<0.01	0.81	<0.01	–
Na_2O	1.60	0.03	0.07	0.07	0.02	n.a.	n.a.	n.a.	n.a.	n.a.	n.a.	–	0.02	0.62	0.39	0.37
K_2O	0.08	n.a.	n.a.	n.a.	n.a.	n.a.	n.a.	n.a.	n.a.	n.a.	n.a.	–	0.02	5.17	0.05	0.10
ZrO_2	n.a.	n.a.	n.a.	n.a.	n.a.	n.a.	0.08	0.09	<0.01	n.a.	n.a.	–	n.a.	0.34	0.02	–
V_2O_3	n.a.	n.a.	n.a.	n.a.	n.a.	n.a.	0.01	0.14	0.27	n.a.	n.a.	–	n.a.	n.a.	<0.01	
Nb_2O_5	n.a.	n.a.	n.a.	n.a.	n.a.	n.a.	<0.01	<0.01	0.01	n.a.	n.a.	–	n.a.	n.a.	<0.01	–
NiO	n.a.	n.a.	n.a.	n.a.	n.a.	<0.01	n.a.	n.a.	n.a.	0.14	0.07	–	n.a.	<0.01	<0.01	–
S	n.a.	n.a.	n.a.	n.a.	n.a.	n.a.	n.a.	n.a.	n.a.	<0.01	37.85	–	n.a.	0.06	0.08	–
F	n.a.	n.a.	n.a.	n.a.	n.a.	n.a.	n.a.	n.a.	n.a.	n.a.	n.a.	2.31	n.a.	n.a.	<0.01	–
Co	n.a.	n.a.	n.a.	n.a.	n.a.	n.a.	n.a.	n.a.	n.a.	0.81	<0.01	–	n.a.	n.a.	<0.01	–
Total	99.92	100.95	99.99	99.73	100.30	100.96	100.15	100.87	100.19	100.38	101.63	100.00	99.17	99.51	100.22	100.31
	An 82.1	Wo 10.1	Wo 20.6	Wo 31.5	Wo 18.3	Fo 70.1							$\frac{Fe}{Fe+Mg}$ = .478		.484	
	Ab 14.0	En 54.5	En 48.8	En 41.7	En 32.3	Fa 29.9										
	Or 0.5	Fs 30.3	Fs 21.9	Fs 14.5	Fs 44.7											
	Others 3.4	5.1	8.7	12.3	4.7											

*Elemental abundances; converted to oxides for calculation of bulk composition.

†Assumed 1:1 mix of fluorapatite and whitlockite.

n.a. = not analyzed.

Table 2: Whole-rock chemistry of 74255.

Sample Method Reference	,25 X,N,I 1	,42 X 2	,25 N,I 3	,155 N 4	C 5	GC 6
SiO_2 (wt%)	37.96	38.4				
TiO_2	12.17	12.76				
Al_2O_3	8.55	8.84				
Cr_2O_3	0.54					
FeO	18.11	17.98				
MnO	0.27					
MgO	9.65	10.72				
CaO	10.59	10.20				
Na_2O	0.36	0.37				
K_2O	0.06	0.10	0.081			
P_2O_5	0.04					
S	0.14				0.1625	
Nb (ppm)		<10				
Zr		310	238	301		
Hf				10.0		
Ta						
U			0.14			
Th						
W						
Y		126				
Sr		165	163			
Rb		1.5	1.22			
Li		8.0	8.3			
Ba		288	71.1			
Cs						
Be		<1				
Zn		5.4				
Pb		4.8				
Cu		36				
Ni		17				
Co		34	22.3			
V		65				
Sc		62	74.2			
La		<10	6.50			
Ce			22.5			
Nd			24.7			
Sm			10.1			

Table 2: (Concluded).

Sample	,25	,42	,25	,155		
Method	X,N,I	X	N,I	N	C	GC
Reference	1	2	3	4	5	6
Eu			1.85			
Gd			15.3			
Tb						
Dy			17.3			
Er			10.0			
Yb		11	8.93			
Lu						
Ga		6.1				
F						
Cl						
C						
N						
H						1.0
He						
Pd (ppb)						
Ge						
Re						
Ir						
Au						
Ru						
Os						

References: 1 = Rhodes et al. (1976); 2 = Rose et al. (1975); 3 = Shih et al. (1975); 4 = Hughes and Schmitt, 1985; 5 = Gibson et al. (1975); 6 = Gibson et al. (1987).

X = XRF; N = INAA; I = Isotope dilution; C = Combustion; GC = Gas Chromatography.

Table 3: Rb-Sr isotopic composition of 74255.

Ref. Sample Mineral	1 ,25 WR	2,3 ,25 WR	2,3 ,25 Plag 1	2,3 ,25 Ilm	2,3 ,25 Ilm + Px1	2,3 ,25 Ilm + Px2	2,3 ,25 Plag 3	4 ,25 WR 1	4 Plag	4 Px 1	4 Px 2	4 Ilm	4 Meso
Wt (mg)	52	52	4.7	8.2	52	24	18	25.48	24.37	24.83	24.12	19.52	1.423
K (ppm)	--	--	--	--	--	--	--	720	1713	491	452	157	3116
Ba (ppm)	--	--	--	--	--	--	--	--	196.6	65.5	70.2	19.4	503
Rb (ppm)	1.22	1.22	0.223	1.92	2.28	2.14	0.222	1.198	2.644	0.9924	0.9591	0.3458	6.795
Sr (ppm)	163	163	514	81.2	99.4	102	556	158.3	546.0	85.97	78	12.28	289.7
$^{87}Rb/^{86}Sr$	0.0217	0.0217	0.00126	0.0684	0.0663	0.0605	0.00115	0.0219	0.0140	0.0334	0.0356	0.0814	0.0678
Error	±3	±3	±3	±5	±5	±5	±1						
$^{87}Sr/^{86}Sr$	0.70045	0.70045	0.69930	0.70285	0.70288	0.70255	0.69931	0.70034	0.69998	0.70092	0.70113	0.70352	0.70278
Error	±6	±6	±5	±19	±7	±10	±16	±8	±11	±7	±18	±10	±19
$T_{BABI}{}^{a}$ (Ga)	4.3	4.34											
Error	±0.3	±0.25											
$T_{LUNI}{}^{b}$ (Ga)	4.6	4.56											
Error	±0.3	±0.25											

References: 1 = Nyquist et al. (1975); 2 = Nyquist et al. (1976); 3 = Bansal et al. (1975); 4 = Murthy and Coscio (1976).

WR = Whole-Rock; Plag = Plagioclase; Ilm = Ilmenite; Px = Pyroxene; Meso = Mesostasis.

a = I(Sr) of 0.69910 (BABI ± JSC bias); b = I(Sr) of 0.69903 (A16 Anorthosites for T = 4.6 Ga)

Table 4: U-Th-Pb isotopic composition of 74255.
Data from Nunes et al. (1974).

wt (mg)	U (ppm)	Th (ppm)	Pb (ppm)	$^{232}Th/^{238}Th$	$^{238}U/^{204}Pb$
207.4	0.1323	0.4451	0.2421	3.48	427

		Observed ratios			Corrected for analytical blank				
wt (mg)	Run	$^{206}Pb/^{204}Pb$	$^{207}Pb/^{204}Pb$	$^{208}Pb/^{204}Pb$	$^{206}Pb/^{204}Pb$	$^{207}Pb/^{204}Pb$	$^{208}Pb/^{204}Pb$	$^{207}Pb/^{204}Pb$	$^{208}Pb/^{206}Pb$
207.4	P	478.1	227.7	441.9	680.7	321.5	621.1	0.4723	0.9125
207.4	C*	431.0	206.7	-----	586.7	278.8	-----	0.4752	-----

	Corrected for blank and primordial Pb				Single stage ages (MA)			
Run	$^{206}Pb/^{238}U$	$^{207}Pb/^{235}U$	$^{207}Pb/^{206}Pb$	$^{208}Pb/^{232}Th$	$^{206}Pb/^{238}U$	$^{207}Pb/^{235}U$	$^{207}Pb/^{206}Pb$	$^{208}Pb/^{232}Th$
C1P	0.8764	55.98	0.4635	0.2222	4,095	4,159	4,190	4,110
C1	0.8745	56.03	0.4650	-----	4,088	4,159	4,194	----

Table 5: Exposure ages of and cosmogenic radionuclide abundances in 74255.

	Reference 1 Sample 74225,18	Reference 2 Sample 74255,18	Reference 3
^{4}He (10^{-8} cm^3 STP/g)	11300 ± 500		11300
^{20}Ne (10^{-8} cm^3 STP/g)	1.7 ± 0.09		1.53
^{40}Ar (10^{-8} cm^3 STP/g)	1700 ± 200		1700
^{86}Kr (10^{-12} cm^3 STP/g)	31 ± 6		31
^{132}Xe (10^{-12} cm^3 STP/g)	19 ± 4		19
^{3}He (10^{-8} cm^3 STP/g)	11.4 ± 0.6		
^{21}Ne (10^{-8} cm^3 STP/g)	1.53 ± 0.09		
^{38}Ar (10^{-8} cm^3 STP/g)	1.63 ± 0.2		
^{83}Kr (10^{-12} cm^3 STP/g)		40 ± 8	

1 = Eugster et al. (1977); 2 = Eberhardt et al. (1975); 3 = Morgelli et al. (1977)